JOURNAL OF GUIDANCE, CONTROL, AND DYNAMICS
Vol. 31, No. 6, November–December 2008

Novel Nonlinear Hammerstein Model Identification: Application to Nonlinear Aeroelastic/Aeroservoelastic System

Jie Zeng* and Dario H. Baldelli†
ZONA Technology, Inc., Scottsdale, Arizona 85258
and
Martin Brenner‡
NASA Dryden Flight Research Center, Edwards, California 93523

DOI: 10.2514/1.35719

In this paper, a novel iterative algorithm for the identification of a nonlinear Hammerstein system is presented. The proposed algorithm is based on the iterative estimation and the orthonormal basis functions. The linear part of the Hammerstein cascade system is represented by the orthonormal finite impulse response filter, and the static nonlinear part is represented by the cubic spline function. The advantage of using orthonormal bases in the orthonormal finite impulse response filter lies in the possibility of incorporating prior poles knowledge of the system dynamics into the identification process. As a result, more accurate and simplified linear models can be obtained with a limited number of basis functions. Using the cubic spline function instead of the polynomial will greatly improve the extrapolation capability of the static identified nonlinearity. Furthermore, a criterion based on the frequency-domain identification method and stabilization diagram is introduced to estimate the physical poles of the dynamic system. Two case studies including a simulated structurally nonlinear prototypical two-dimensional wing section are presented to illustrate the proposed identification algorithm.

Nomenclature

$A(\omega)$ = denominator matrix polynomial
a = elastic axis location of the model
$B(\omega)$ = numerator matrix polynomial
$B_i(q)$ = orthonormal basis function
b = half-chord length
C = damping matrix
c_h = plunge structural damping coefficient
$c_{l\alpha}$ = aerodynamic lift coefficient due to pitch angle
$c_{l\beta}$ = aerodynamic lift coefficient due to flap
$c_{m\alpha}$ = aerodynamic moment coefficient due to pitch angle
$c_{m\beta}$ = aerodynamic moment coefficient due to flap
c_α = pitch structural damping coefficient
$f(\alpha)$ = static nonlinear function
$G(q)$ = linear time invariant function
$G(\omega)$ = frequency response function
h = plunge variable
I_α = mass moment of inertia about the elastic axis
K = stiffness matrix
k_h = structural stiffness
$k_\alpha(\alpha)$ = torsional stiffness
M = mass matrix
m_T = total mass of wing and its support structure
m_w = total mass of the wing only
N = data length
$N(\cdot)$ = zero memory static nonlinear function
P = augmented nominal linear pant
$P(q)$ = all pass transfer function
q = forward shift operator
U = freestream velocity
$u(t)$ = input signal
$V_N(\theta)$ = cost function
x_a = nondimensionalized distance between the center of mass and elastic axis
$y(t)$ = output signal
$\alpha(t)$ = pitch variable
β_i = orthonormal basis coefficients
$\beta(t)$ = flap deflection
γ_k = cubic spline coefficients
Δ_T = sampling time
θ = unknown parameters to be estimated
θ_l = unknown linear parameters to be estimated
θ_n = unknown nonlinear parameters to be estimated
λ = standard deviation
$\nu(t)$ = external Gaussian noise
ω = frequency variable

Subscript

i = variable index
j = frequency point index
k = parameter index

I. Introduction

A HAMMERSTEIN model is a block-oriented nonlinear model, which consists of a static nonlinearity followed by a linear time invariant system. It has been successfully used to represent nonlinear systems in some practical applications within the area of process engineering [1], biomedical engineering [2,3], and aeroelastic engineering [4].

In the last decades, extensive research has been reported in the literature for the identification of the Hammerstein models. The most popular identification algorithm for the Hammerstein model is the Narendra-Gallman (NG) algorithm [5]. The NG algorithm separates the parameters into two sets, a linear parameters set and a nonlinear parameter set. During the estimation process, one set is calculated whereas the other set is fixed, and vise versa. The estimation stops when it converges. An alternative one is a correlation technique [6], which relies on a separation assumption. This method only works if the input is Gaussian white noise. In the separable least-squares (SLS)

Presented as Paper 6302 at the AIAA Atmospheric Flight Mechanics Conference and Exhibit, Hilton Head, SC, 20–23 August 2007; received 16 November 2007; revision received 13 March 2008; accepted for publication 14 March 2008.

*Research and Development Control System Engineer. Member AIAA.
†Control and Aeroservoelastic Manager. Senior Member AIAA.
‡Aerospace Engineer. Senior Member AIAA.

approach [2,3,7,8], the parameters of the linear part and those of the nonlinear part can be estimated separately due to one set of parameters being written as a function of the other set. The non-iterative subspace identification method is extended from linear system identification cases to nonlinear identification cases [9], which also assumes a Gaussian white noise input. Recent advances are proposed [10,11], which are based on least-squares estimation, singular value decomposition, and/or orthonormal bases and another [3] that relies on the SLS optimization method and cubic spline functions.

In this paper, a novel iterative algorithm is proposed based on the previous achievements on the identification techniques of Hammerstein models. This method can be further extended to deal with the more complex Wiener models. In the proposed algorithm, orthonormal bases are applied to parameterize the linear part of the Hammerstein system, and a cubic spline is chosen to represent the static nonlinear part of the dynamic system. With the use of the orthonormal base expansions, the prior poles information of the dynamic system can be incorporated. Therefore, the iterative algorithm converges fast and is very efficient.

Using orthonormal bases to parameterize dynamic systems has been widely applied in model estimation techniques [12,13]. In the constructions of the orthonormal basis functions, Laguerre and Kautz bases have been used successfully in system identification and signal processing [14,15]. A unifying construction [16] generalized both the Laguerre and Kautz bases in the context of system identification. A further generalization of these results for arbitrary dynamic systems was reported in [17]. It has been shown [17] that if the dynamics of the orthonormal basis functions approach the dynamics of the system to be approximated, the convergence rate of the affine series expansion will increase, and as a result the number of parameters to be determined to accurately approximate the system will be much smaller. Therefore, the iteration process of the proposed method will closely depend on the tuning of the orthonormal bases.

The most common way to create the orthonormal basis functions is to estimate a low-order model from experimental data, using standard open loop identification algorithms such as the output error (OE) identification method [18]. This low-order model can usually catch the most important dynamics of the estimated dynamic system, and from this low-order model some poles can be extracted to generate the set of orthonormal basis functions. However, this low-order model may still miss some important dynamics of the dynamic system, and the system approximation using orthonormal basis function expansion will be biased. In this paper, a criterion using a frequency-domain identification methodology and stabilization diagram will be introduced to estimate the possible physical poles of the dynamic system. With this criterion, the physical poles can be consistently estimated, and thus used to generate the set of orthonormal basis functions.

The main contributions of the paper are as follows:

1) A new iterative identification algorithm is derived from a Hammerstein model. With the use of the iterative algorithm, the estimation is separated into two simple easy-handle standard linear least-squares estimations, and the dimension of the optimization space is reduced. As a result, a better numerical conditioning could be obtained compared with its nonseparable counterpart.

2) Using the cubic spline functions instead of the polynomial functions to represent the piecewise static nonlinearity provides much better signal extrapolation capability.

3) With the implementation of the frequency-domain PolyMax identification method and the stabilization diagram, the physical poles information of the dynamic system can be consistently extracted. Injecting these estimated poles into the orthonormal finite impulse response filter results in an accurate and low-order linear model.

This paper is outlined as follows. Following the problem formulation in Sec. II, Sec. III will describe the techniques regarding the generation of the orthonormal basis functions. A frequency-domain identification method is presented in Sec. IV to estimate the physical poles of the dynamic system, and an iterative estimation algorithm is discussed in Sec. V. Two case studies in Sec. VI will illustrate the performance of the proposed nonlinear Hammerstein model identification algorithm.

II. Problem Formulation

A Hammerstein model is represented in Fig. 1. The model consists of a zero memory static nonlinear function $N(\cdot)$ in cascade with a linear time invariant function $G(q) \in \mathcal{RH}_2$. Here $v(t)$ is assumed to be an independently and identically distributed Gaussian noise, which is added to the output $y(t)$. The input and output relationship is given as

$$y(t) = G(q)N(u(t)) + v(t) \tag{1}$$

The objective is to identify the nonlinear function $N(\cdot)$ and the linear function $G(q)$ based on the measured input/output data segment $\{u(t), y(t)\}_{t=0}^{N}$. The nonlinear function $N(\cdot)$ can be parameterized by polynomial or cubic spline functions. It should be mentioned that only a certain class of nonlinear function $N(\cdot)$ such as saturation, free play, and hyperbolic tangent, can be approximated by polynomial or cubic spline. For a complicated static nonlinear function, other expressions to represent such a nonlinearity should be proposed.

Using polynomial functions to approximate the nonlinear function $N(\cdot)$ and the orthonormal basis to approximate the linear part $G(q)$ and its application to identify the nonlinear aeroelastic/aeroservoelastic model has been previously investigated [4]. Even though polynomial functions can be used to represent nonlinear systems in some cases, it is known that they have several drawbacks compared with the cubic spline functions. Among them are 1) characteristic oscillatory behavior of high-order polynomial, 2) bad extrapolation behavior, and 3) numerical problem with high-order polynomial. Therefore, in this paper, the emphasis of the use of cubic spline functions is given to estimate the nonlinear function $N(\cdot)$. For completeness, a comparison between polynomial representation and cubic spline representation is also performed in this paper.

The cubic spline function [1] has the form

$$v(t, \theta_n) = \sum_{k=2}^{m-1} \gamma_k |u - w_k|^3 + \sum_{k=m}^{m+3} \gamma_k u^{k-m} \tag{2}$$

where $\theta_n = \{\gamma_2, \gamma_3, \ldots, \gamma_{m+3}\}$ are the parameters needed to be estimated via a properly chosen system identification algorithm. Here w_k is a set of knots $\{w_1, \ldots, w_m\}$ and is defined as

$$u_{\min} = w_1 < w_2 < w_3 \cdots < w_m = u_{\max}$$

Alternatively, a polynomial function representation for the static map can be given as

$$v(t, \theta_n) = \sum_{k=1}^{n} \gamma_k u^k \tag{3}$$

The linear system $G(q)$ can be expressed as a linear expansion of orthonormal basis functions and is given as

$$G(q, \theta_l) = \sum_{i=0}^{N-1} \beta_i B_i(q) \tag{4}$$

where $B_i(q)$ is the set of basis functions generated from the a priori poles information of the dynamic system, and $\theta_l = \{\beta_0, \ldots, \beta_{N-1}\}$ are the parameters to be identified.

Substitute Eq. (4), and Eq. (2) into Eq. (1), and the input and output relationship can be rewritten as

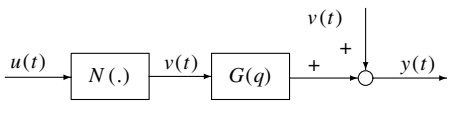

Fig. 1 Hammerstein system.

$$y(t) = \left[\sum_{i=0}^{N-1} \beta_i B_i(q)\right] \cdot \left[\sum_{k=2}^{m-1} \gamma_k |u - w_k|^3 + \sum_{k=m}^{m+3} \gamma_k u^{k-m}\right] + \nu(t) \tag{5}$$

III. Generation of Orthonormal Basis Functions

The application of orthonormal basis functions to parameterize and estimate a dynamic system has obtained extensive attention in recent years. Different constructions of the orthonormal basis structure have been reported in [16,17,19]. In this section, it is assumed that the pole locations have already been estimated with the use of the standard open loop prediction error system identification methods. Suppose the poles $\{\xi_i\}$ $(i = 1, 2, \ldots, N)$are known, an all pass function $P(q)$ created by these poles is given as

$$P(q) = \prod_{i=1}^{N} \left[\frac{1 - \xi_i^* q}{q - \xi_i}\right] \tag{6}$$

Let (A, B, C, D) be the minimal balanced realization of the all pass function $P(q)$, define the input to state transfer function $B_0(q) = (qI - A)^{-1}B$, then a set of functions $B_i(q)$ can be obtained via

$$B_i(q) = B_0(q)P^i(q) \tag{7}$$

and $B_i(q)$ has the orthogonal property

$$\frac{1}{2\pi j} \oint B_i(q) B_k^T\left(\frac{1}{q}\right) \frac{\mathrm{d}q}{q} = \begin{cases} I & i = k \\ 0 & i \neq k \end{cases} \tag{8}$$

The construction of the orthonormal basis function is illustrated in Fig. 2.

It should be noted that if $B_0(q)$ includes all the poles information of a dynamic system, then only one parameter β_0 needs to be estimated to approximate this dynamic system. It means that the parameters estimated will directly depend on the a priori system information injected into the basis functions B_i.

IV. Physical Modes Estimation

In Sec. III, the generation of the orthonormal basis function depends on the pole locations of the dynamic system, which, in most cases, is unknown. Furthermore, as mentioned before, the accuracy of model estimation relies on the orthonormal basis functions B_i, which again relies on the accuracy of the poles injected into the basis functions B_i. A technique [20] combining the frequency-domain PolyMax methodology and the stabilization diagram concept is proposed to estimate the physical poles of the dynamic system. A brief description of the proposed technique is presented here.

Assuming a set of noisy complex frequency response functions (FRF) measurement data $G(\omega_j)$ $(j = 1, \ldots, N)$, the approximation of the data by a model, $P(\omega)$, is addressed by considering the following additive error:

$$E(\omega_j) = G(\omega_j) - P(\omega_j) \qquad j = 1, \ldots, N \tag{9}$$

Then, it is assumed that the model $P(\omega)$ can be represented by a right polynomial fraction matrix given by

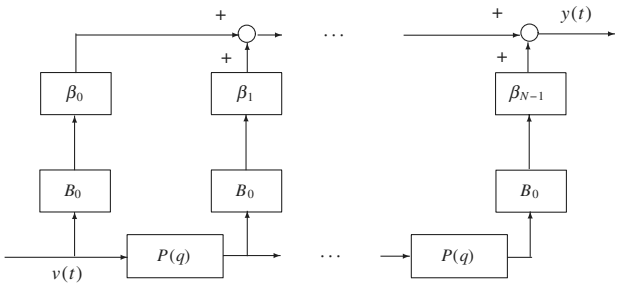

Fig. 2 Construction of orthonormal basis function.

$$P(\omega) = [B(\omega)][A(\omega)]^{-1} \tag{10}$$

where $P(\omega) \in \mathcal{C}^{p \times m}$ is the FRF matrix with p outputs and m inputs, $B(\omega) \in \mathcal{C}^{p \times m}$ is the numerator matrix polynomial, and $A(\omega) \in \mathcal{C}^{m \times m}$ is the denominator matrix polynomial.

For a model having m inputs and p outputs, each row of the right matrix fraction model can be written as

$$P_i(\omega) = [B_i(\omega)][A(\omega)]^{-1} \qquad i = 1, 2, \ldots, p \tag{11}$$

where the polynomial matrix $B_i(\omega)$ is parameterized by

$$B_i(\omega) = \sum_{k=0}^{n_b} B_{ik} \xi_k(\omega) \tag{12}$$

where $B_{ik} \in \mathcal{R}^{1 \times m}$. In addition, n_b are the number of nonzero matrix coefficients in $B(\omega)$ or the order of $B(\omega)$, and $\xi_k(\omega)$ are the polynomial basis functions. For the continuous time model, $\xi_k(\omega) = -i\omega_k$. For the discrete-time model, $\xi_k(\omega) = e^{-i\omega_k T}$, with T as the sampling time. In what follows, only the discrete-time case will be considered.

The polynomial matrix $A(\omega)$ is parameterized by

$$A(\omega) = \sum_{k=0}^{n_a} A_k \xi_k(\omega) \tag{13}$$

where $A_k \in \mathcal{R}^{m \times m}$, and n_a are the number of nonzero matrix coefficients in $A(\omega)$.

Defining

$$\beta_i = [B_{i0}, B_{i1}, \ldots, B_{in_b}] \in R^{(n_b+1) \times m} \qquad i = 1, 2, \ldots, p$$

the polynomial matrix coefficients $\beta_i \in \mathcal{R}^{(n_b+1) \times m}$ and $A_k \in \mathcal{R}^{m \times m}$ are stacked in the following way for computational purposes:

$$\theta = [\beta_1, \ldots, \beta_p; A_0, \ldots, A_{n_a}] \tag{14}$$

where the parameter θ is the unknown coefficient that needs to be estimated. Based on the framework of the least-squares approach, the linear least-squares equation error is obtained by right multiplying $A(\omega)$ in Eq. (11), which yields

$$\varepsilon_i(\omega) = W_i(\omega)[B_i(\omega) - G_i(\omega)A(\omega)] \tag{15}$$

where W_i is a scalar weighting function for each output. The parameter θ is calculated by minimizing the cost function $V(\theta)$

$$\hat{\theta} = \arg\min_{\theta}[V(\theta)] = \arg\min_{\theta} \sum_{i=1}^{p} \sum_{k=1}^{N} \mathrm{tr}\{\varepsilon_i(\omega_k, \theta)^H \varepsilon_i(\omega_k, \theta)\} \tag{16}$$

In general, a constraint $A_0 = I_m$ is set to obtain a stable model to fit the measured frequency-domain data. Here, a constraint $A_{n_a} = I_m$ is adopted to extract physical modes from the measured frequency-domain data [21]. With $A_{n_a} = I_m$, the poles of the estimated model are separated into *stable physical* poles and *unstable mathematical* poles, from which a very clean stabilization diagram can be obtained, and the *physical* modal parameters of the real system can be estimated from a quick evaluation of the generated stabilization diagram [22].

The stabilization diagram assumes an increasing model order (number of poles noted in the ordinate axis), and it indicates where on the frequency axis the poles are located. As a rule, unstable poles and stable real poles are not considered in the plot. Physical modes should appear as *stable* complex conjugate poles, independent of the number of the assumed model order. On the other hand, *mathematical* poles that intent to model the noise embedded on the data will probably change with the assumed model order. An illustration of how to obtain physical poles from stabilization diagram is shown by a four-mode example in Fig. 3. From Fig. 3a, it is shown that by choosing $A_{n_a} = I_m$, four complex conjugate poles are consistently estimated regardless of the change of the model

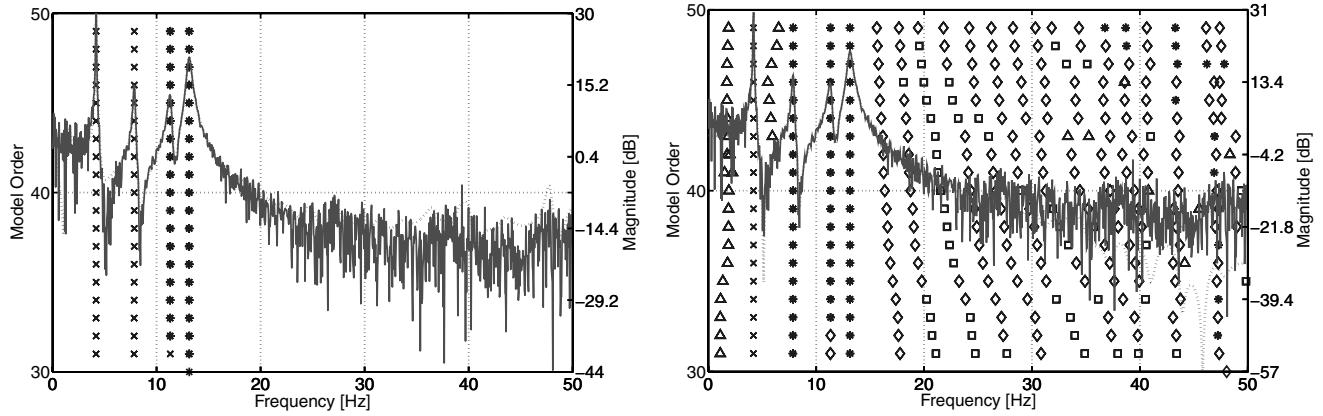

a) Stabilization diagram with $A_{n_0} = I_m$ **b) Stabilization diagram with $A_{n_0} = I_m$**

Fig. 3 Illustration of stabilization diagram using PolyMax identification method.

order. However, with $A_{n_0} = I_m$, the physical poles cannot be easily obtained from the corresponding stabilization diagram, which is shown in Fig. 3b. The estimation results from accessing the stabilization diagram in Fig. 3a are further illustrated in Table 1.

In Table 1, the second column indicates the frequency and damping of the true modes. The third column presents the estimated frequency and damping of the true modes using the proposed PolyMax identification method and stabilization diagram. Comparing the estimated modes and true modes in Table 1, it is obvious to see that the frequency f_i and damping ζ_i $(i = 1, 2, 3, 4)$of these four physical modes are estimated consistently.

V. Identification Algorithm

The cost function used for the parameter estimation can be given as

$$V_N(\theta) = ||\varepsilon(\theta)||_2^2 = ||y(t) - \hat{y}(t, \theta)||_2^2 \tag{17}$$

where $\theta = [\theta_n, \theta_l]$. The parameters θ are estimated by minimizing

$$\hat{\theta} = \arg\min_{\theta}\{V_N(\theta)\} \tag{18}$$

Because the parameters enter the output linearly, an iterative estimation approach is applied to solve the minimization of cost function $V_N(\theta)$. The detail of the iterative algorithm are described as follows:

Initialization:

1) Let $N(u) = u$, then estimate the linear parameters θ_l^0 using the linear least-squares algorithm. Build $G(\theta_l^0, q)$ based on the estimated linear parameters θ_l^0 and Eq. (4).

2) Filtering the input with the estimated linear function $G(\theta_l^0, q)$, estimate the nonlinear parameters θ_n^0 using the linear least-squares algorithms again.

Iteration: Denote θ_l^i and θ_n^i are estimated from the iteration i, then

1) Estimate the linear parameter θ_l^{i+1} given θ_n^i by minimizing cost function

$$V_N(\theta_l^{i+1}, \theta_n^i) = \|y(t) - \hat{y}(t, \theta_l^{i+1}, \theta_n^i)\|_2^2 \tag{19}$$

2) Estimate the nonlinear parameter θ_n^{i+1} given θ_l^{i+1} by minimizing cost function

$$V_N(\theta_l^{i+1}, \theta_n^{i+1}) = \|y(t) - \hat{y}(t, \theta_l^{i+1}, \theta_n^{i+1})\|_2^2 \tag{20}$$

The iteration stops if the cost function $V_N(\theta)$ converges to a steady value or the value decreases at a very slow rate.

A detailed convergence analysis of the iterative Hammerstein identification algorithm is performed in [23]. It was stated that, for a FIR Hammerstein model, by normalizing the iterative algorithm, the iterative algorithm is convergent if it starts from a certain set of initial conditions that are fixed, available before identification and independent of the systems to be estimated. Moreover, under certain conditions, the algorithm converges to the true values in one step. The convergence analysis method indicated in [23] can further be extended to account the orthonormal Hammerstein model presented in this paper. An asymptotic property analysis of Hammerstein model estimates can be found in [24]. Furthermore, the accuracy of the linear model estimation of a nonlinear Hammerstein system is investigated in [25]. The key point in [25] is that the process of estimating the nonlinear part can have a significant effect on the associate estimate of the linear model.

Table 1 Comparison between the identified modes and true modes

	True modes	Identified modes
f_1, Hz	4.1866	4.1868
f_2, Hz	7.8648	7.8630
f_3, Hz	11.3191	11.3303
f_4, Hz	13.1320	13.1320
ζ_1, %	0.5261	0.5622
ζ_2, %	0.9883	1.1035
ζ_3, %	1.4224	1.4836
ζ_4, %	1.6502	1.6333

VI. Case Study

To illustrate the capabilities of the proposed identification algorithm, two case studies are analyzed in the following sections. In the first case study, the simulated data comes from a standard unknown nonlinear Hammerstein system. It will be used to demonstrate the proposed Hammerstein model identification algorithm in this paper. The second case study is an aeroelastic

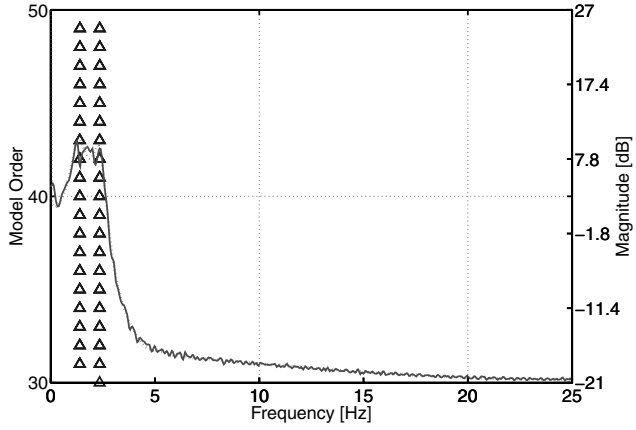

Fig. 4 Stabilization diagram.

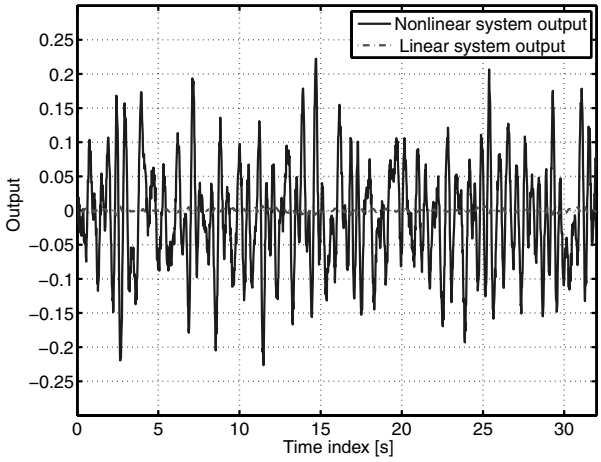

a) Fit of response

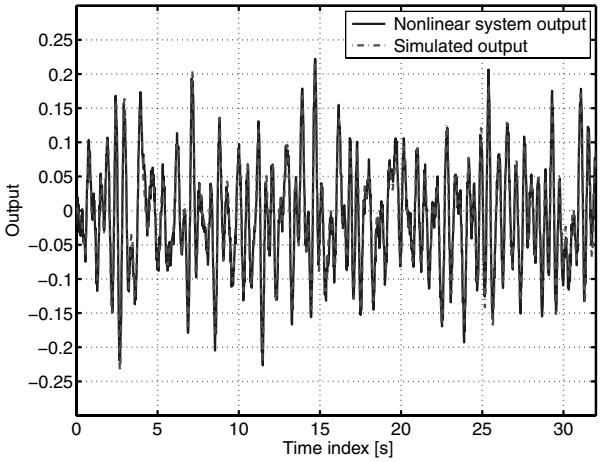

b) Fit of response

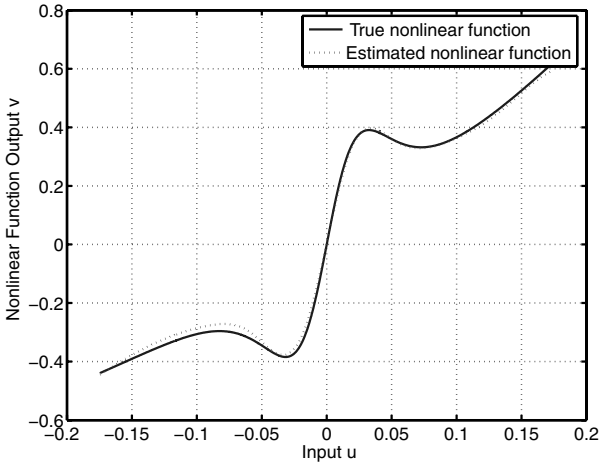

c) Fit of nonlinear function with 10 knots

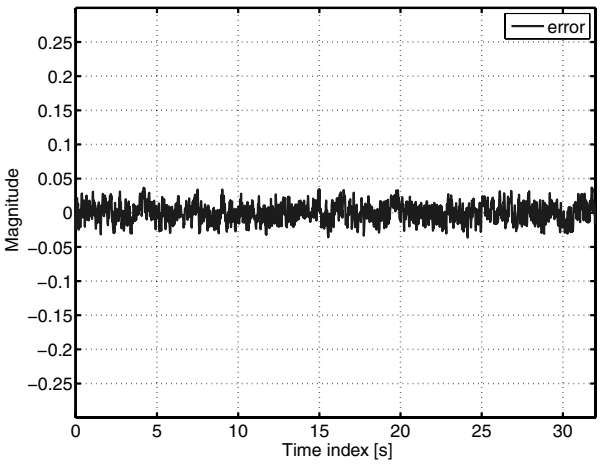

d) Error

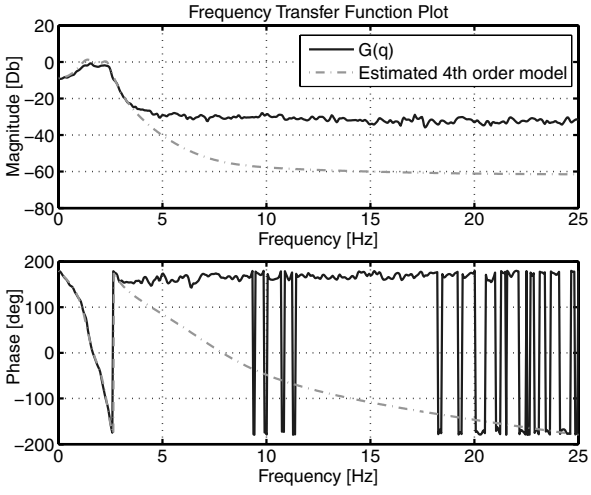

e) Fit of linear model *G(q)*

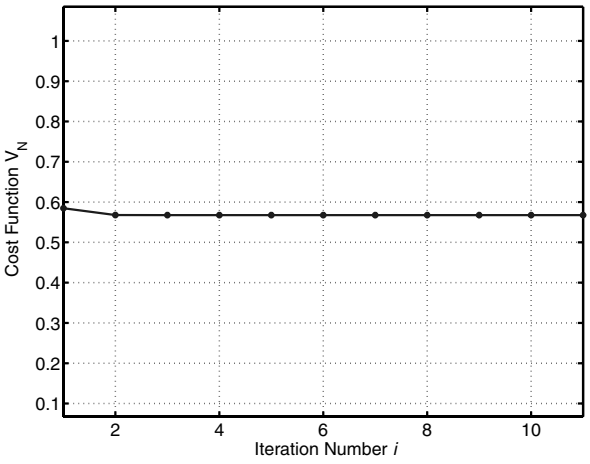

f) Cost function

Fig. 5 Nonlinear Hammerstein model estimation.

pitch-plunge system. This system is composed of a rigid airfoil, whose motion is restricted to pitch and plunging, mounted in a wind tunnel facility. It mimics the Texas A&M University wind tunnel model [26].

A. Case Study 1: Nonlinear Hammerstein System

Consider the simulated process

$$y(t) = G(q)f[u(t)] + v(t) \tag{21}$$

with

$$G(q) = \frac{0.0014583(q+0.9071)(q-0.62470)(q-1.901)}{(q^2-1.889q+0.9216)(q^2-1.863q+0.9491)} \cdot \frac{0.183}{q-0.183} \tag{22}$$

$$f[u(t)] = \tanh[40u(t)] - \tanh[20u(t)] + u^2 + 3u^2 + 3u \tag{23}$$

Table 2 Pitch-plunge system parameters

Parameter	Value
a	−0.6 m
b	0.135 m
$m_{T,w}$	12.387 kg
I_α	0.065 m^2 kg
c_α	0.180 m^2 kg/s
c_{l_α}	6.28
c_{l_β}	3.358
U	10 m/s
k_{α_0}	2.82 Nm/ deg
ρ	1.225 kg/m^3
x_α	0.2466 m
k_h	2844.4 N/m
c_h	27.43 kg/s
c_{m_α}	−0.628
c_{m_β}	−0.635

$$v(t) = \frac{k_m \cdot 0.8q}{q - 0.2} e(t) \tag{24}$$

where the input signal $u(t)$ is chosen as random white Gaussian noise with zero mean; standard deviation $\lambda = 1$. $e(t)$ is a white Gaussian noise; k_m is a constant that is used to obtain a signal to noise ratio of 10% in power at output; and sampling time ΔT is given as $\Delta T = 0.02$.

Using the technique described in Sec. IV, two complex conjugate poles are estimated, using the PolyMax identification method, and extracted from the stabilization diagram, shown in Fig. 4. These poles are calculated as

$$p_{1,2} = 0.9271 \pm 0.2865i \qquad p_{3,4} = 0.9476 \pm 0.1610i \tag{25}$$

and they will be used to generate the orthonormal basis functions shown in Sec. III. As a result, a fourth order all pass function, $P(q)$, is created to generate the basis functions, $B_i(q)$. It should be noted here that it is possible to estimate all physical poles including the real pole $p_5 = 0.183$ using the PolyMax identification method. From Fig. 4 it is observed that the estimated model (red line) and match the frequency response function (green line). The reason only stable complex conjugate poles are extracted during the estimation process is that these poles have crucial effects on the system dynamics compared with real poles. Furthermore, from the control point of view, it is not necessary to estimate such a complicated high-order model for future control design usage. A simplified approximated model including the essential dynamics will suffice.

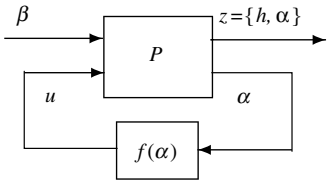

Fig. 6 Nonlinear LFT feedback framework.

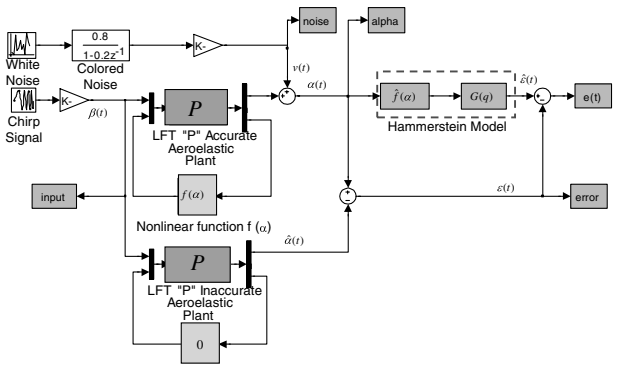

Fig. 7 Simulink model.

In this case study, the parameters that need to be identified during the estimation are chosen as $\theta_l = \{\beta_0\}$ and $\theta_n = \{\gamma_2, \ldots, \gamma_{13}\}$.

Following the identification algorithm in Sec. V, the estimation results are shown in Fig. 5. Figure 5a shows the comparison of the true linear system simulation output and the nonlinear system output; Fig. 5b shows the comparison of the nonlinear system estimation output and the nonlinear system output; Fig. 5c shows comparison plot of the true nonlinear function and the estimated nonlinear function; Fig. 5d shows the plot of the unmodeled error, which is defined as the difference between the nonlinear simulated output and the nonlinear system output shown in Fig. 5b; Fig. 5e shows the comparison of the estimated linear model and the true linear system $G(q)$; Fig. 5f is the plot of the cost function V_N as the function of iteration number i.

The slight mismatch between the estimated linear model and the true linear system, $G(q)$ in high-frequency range, shown in Fig. 5e, is due to the fact the fifth-order true linear system, $G(q)$ is underestimated by a fourth-order orthonormal FIR model. For a more accurate approximation, increasing the order of the estimated orthonormal FIR model is required.

From Fig. 5, it is observed that with a consistent estimation of the physical poles and proper choice of the basis functions, the identification process converges after the second iteration, and the simulated nonlinear output can match the system output. Furthermore, the estimated nonlinear function can consistently fit the true nonlinearity of the dynamics system.

B. Case Study 2: Nonlinear Pitch-Plunge Aeroelastic System

In this case study, a structurally nonlinear prototypical two-dimensional wing section [26] is selected to demonstrate the Hammerstein model identification procedure. The dynamics of the system are described with a high degree of accuracy using the following aeroelastic Equation of Motions (EoMs)

$$\begin{bmatrix} m_T & m_w x_\alpha b \\ m_w x_\alpha b & I_\alpha \end{bmatrix} \begin{bmatrix} \ddot{h} \\ \ddot{\alpha} \end{bmatrix} + \begin{bmatrix} c_h & 0 \\ 0 & c_\alpha \end{bmatrix} \begin{bmatrix} \dot{h} \\ \dot{\alpha} \end{bmatrix} + \begin{bmatrix} k_h & 0 \\ 0 & k_\alpha(\alpha) \end{bmatrix} \begin{bmatrix} h \\ \alpha \end{bmatrix} = \bar{q} 2b \begin{bmatrix} c_{l_\alpha}\left(\alpha + \frac{1}{U}\dot{h} + \left(\frac{1}{2} - a\right) b \frac{1}{U}\dot{\alpha}\right) + c_{l_\beta}\beta \\ c_{m_\alpha}\left(\alpha + \frac{1}{U}\dot{h} + \left(\frac{1}{2} - a\right)\frac{b}{U}\dot{\alpha}\right) + c_{m_\beta}\beta \end{bmatrix} \tag{26}$$

where torsional stiffness $k_\alpha(\alpha)$ is a nonlinear function of the pitch angle α, and $k_\alpha(\alpha) = k_{\alpha_0} + f_1(\alpha)$. The system parameters used in the numerical simulation are given in Table 2.

Defining

$$M = \begin{bmatrix} m_T & m_w x_\alpha b \\ m_w x_\alpha b & I_\alpha \end{bmatrix},$$

$$C = \begin{bmatrix} c_h - 2\bar{q} c_{l_\alpha} \frac{b}{U} & -2\bar{q} c_{l_\alpha}\left(\frac{1}{2} - a\right)\frac{b^2}{U} \\ -2\bar{q} c_{m_\alpha}\frac{b}{U} & c_\alpha - 2\bar{q} c_{m_\alpha}\left(\frac{1}{2} - a\right)\frac{b^2}{U} \end{bmatrix},$$

$$K = \begin{bmatrix} k_h & -2\bar{q} b c_{l_\alpha} \\ 0 & k_{\alpha_0} - 2\bar{q} c_{m_\alpha} \end{bmatrix}, \qquad F_1 = \begin{bmatrix} 2\bar{q} b c_{l_\beta} \\ 2\bar{q} b c_{m_\beta} \end{bmatrix},$$

$$F_2 = \begin{bmatrix} 0 \\ -1 \end{bmatrix}, \qquad x = \begin{bmatrix} h \\ \alpha \end{bmatrix} \tag{27}$$

By substituting Eq. (27) into Eq. (26), the transformed equations of motions in the state space form become

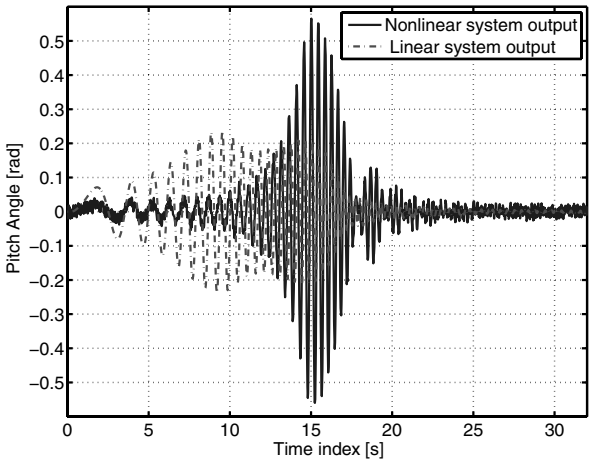

a) Fit of response

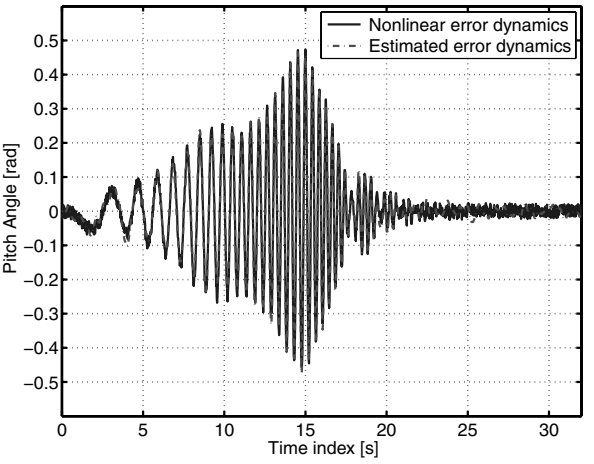

b) Fit of unmodelled dynamics

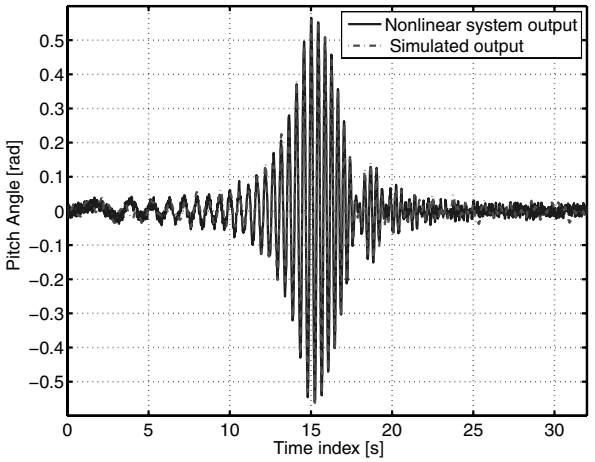

c) Fit of response

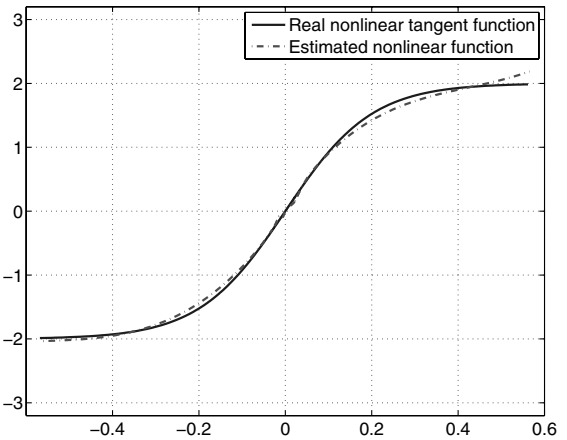

d) Cubic nonlinear function with 13 kt

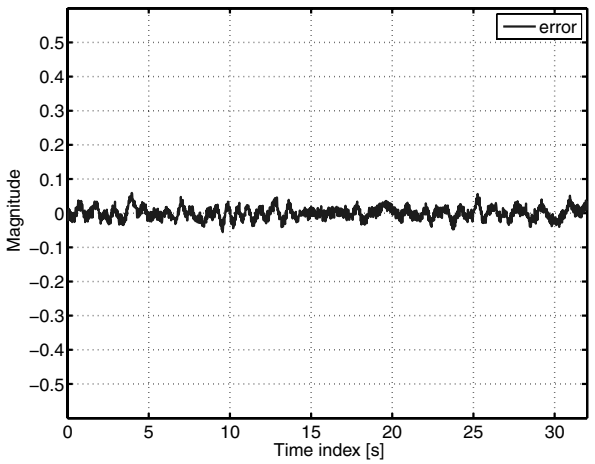

e) Error

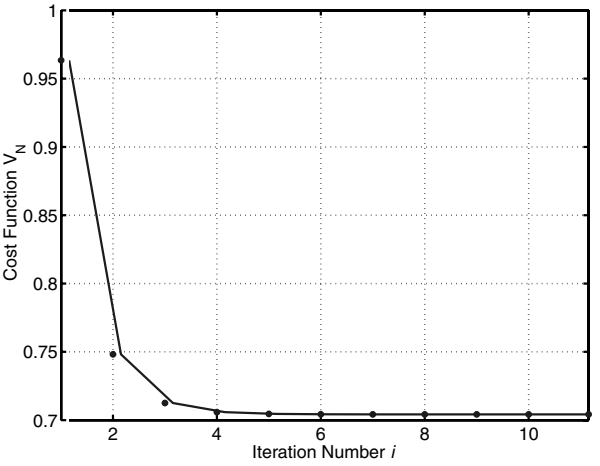

f) Cost function

Fig. 8 Nonlinear model estimations using a cubic spline represent hyperbolic tangent nonlinear representation.

$$\begin{bmatrix}\dot{x}\\ \ddot{x}\end{bmatrix}=\begin{bmatrix}0 & I\\ -M^{-1}K & -M^{-1}C\end{bmatrix}\begin{bmatrix}x\\ \dot{x}\end{bmatrix}+\begin{bmatrix}0\\ M^{-1}F_1\end{bmatrix}\beta + \begin{bmatrix}0\\ M^{-1}F_2\end{bmatrix}f_1(\alpha)\alpha \tag{28}$$

Defining $f(\alpha)=f_1(\alpha)\alpha$, the dynamic system described in Eq. (28) can be easily reformulated in a nonlinear feedback framework using a lower linear fractional transformation (LFT), which is shown in Fig. 6.

From Fig. 6, it is obtained that

$$z=F_l[P,f(\alpha)]\beta \qquad P=\begin{bmatrix}P_{11} & P_{12}\\ P_{21} & P_{22}\end{bmatrix} \tag{29}$$

$f(\alpha)$ in Eq. (29) is a static nonlinear function of the states $\alpha(t)$, and P is the augmented nominal linear plant. Given the framework in Eq. (29), the pitch angle $\alpha(t)$ can be written as

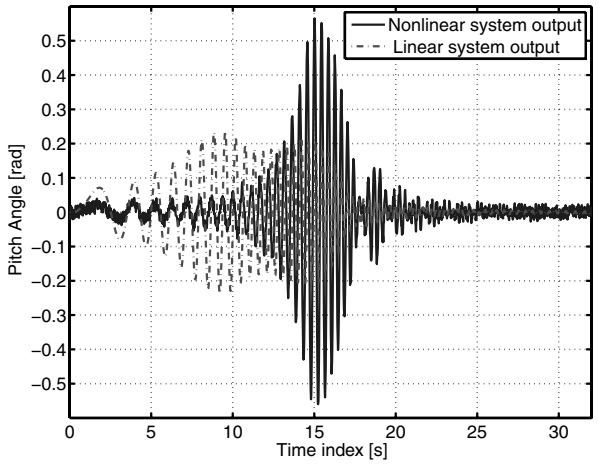

a) Fit of response

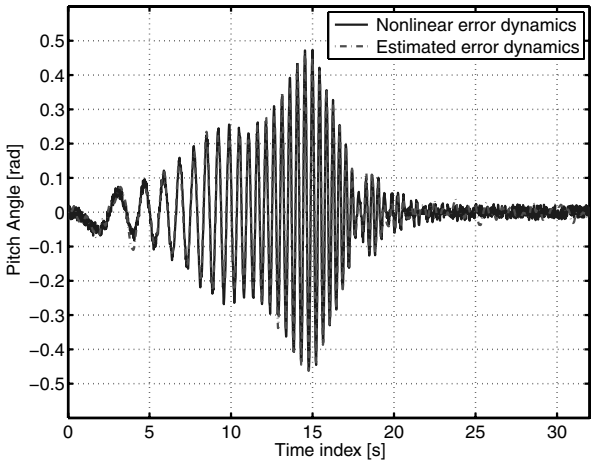

b) Fit of unmodelled dynamics

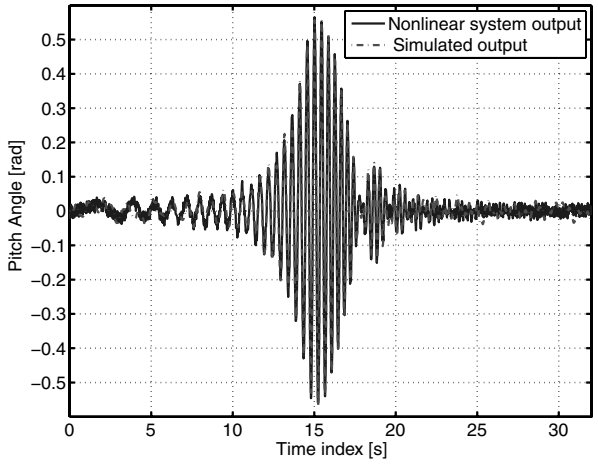

c) Fit of response

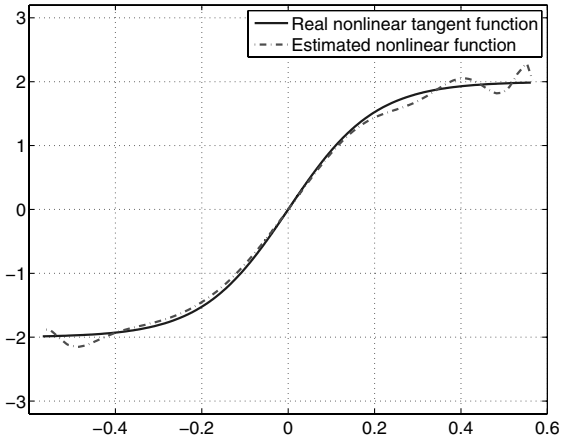

d) 15th–order polynomial nonlinear function

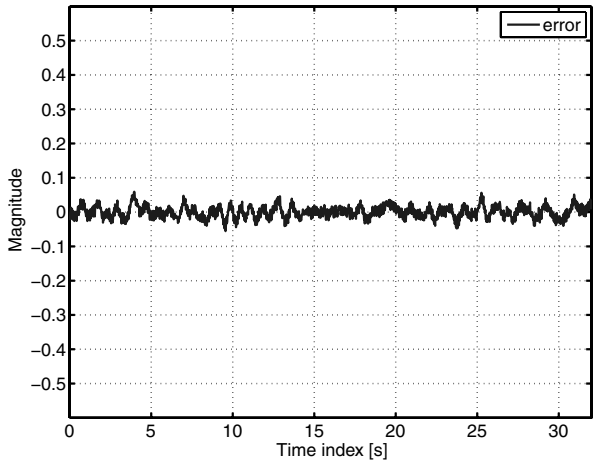

e) Error

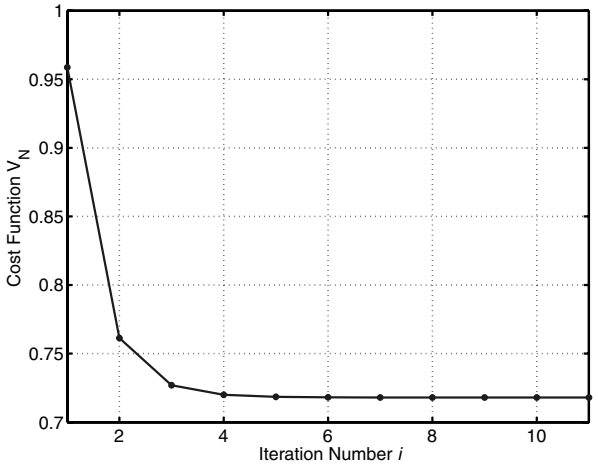

f) Cost function V_N

Fig. 9 Nonlinear model estimations using a polynomial represent real hyperbolic tangent nonlinear representation.

$$\alpha = P_{21}\beta + P_{22}f(\alpha) \tag{30}$$

if P_{21} is known and β and α are the measured input/output signals, then P_{22} and the static nonlinear function $f(\alpha)$ can be estimated using Hammerstein model estimation from the input α to the error dynamics $\alpha - P_{21}\beta$.

The Simulink model is shown in Fig. 7. The simulated nonlinear system output is the pitch angle $\alpha(t)$, which is corrupted with a zero-mean Gaussian distributed white noise with standard deviation $\sigma = 0.01$, and the system input is the flap deflection $\beta(t)$. The error signal $\varepsilon(t)$ is defined as the difference between the noise corrupted nonlinear output $\alpha(t)$ and the linear model output $\hat{\alpha}(t)$. The Hammerstein nonlinear identification algorithm is applied to identify the unmodeled dynamics from an N point data set $\{\alpha(t), \varepsilon(t)\}$. In this simulation, the sampling frequency is chosen as 50 Hz because the main frequency content of the physical system is below 3 Hz.

To demonstrate the advantage of using the cubic spline function to represent the static nonlinearity, a hyperbolic tangent function is used in this case study to represent the nonlinear function $f(\alpha)$ instead of a polynomial function used in [26]. If the true nonlinearity is a

polynomial function, it is not necessary to use the cubic spline function. The hyperbolic tangent function is given as

$$u = f(\alpha) = 2 \cdot \tanh(5\alpha)$$

The poles used to generate the orthonormal basis function are estimated again with the PolyMax method described in Sec. IV. They are complex conjugate poles, given as

$$p_{1,2} = 0.9312 \pm 0.2849i \qquad p_{3,4} = 0.9470 \pm 0.1596i \qquad (31)$$

Defining the parameters to be estimated for the unknown nonlinear Hammerstein system as $\theta_l = \{\beta_0\}$ and $\theta_n = \{\gamma_2, \ldots, \gamma_{16}\}$, using the poles in Eq. (31), following the orthonormal basis function generation in Sec. III, and the identification algorithm in Sec. V, the estimation results are shown in Fig. 8.

Figure 8a shows the comparison of the true linear system simulation output and the nonlinear system output; Fig. 8b shows the comparison of the output of the estimated nonlinear error dynamics and the output of the nonlinear error dynamics; Fig. 8c shows the comparison of the nonlinear system estimation output and the nonlinear system output; Fig. 8d shows the comparison of the true nonlinear tangent function and estimated nonlinear function; Fig. 8e is the plot of the unmodeled error, which is defined as the difference between the nonlinear simulated output and the nonlinear system output shown in Fig. 8c; Fig. 8f is the plot of the cost function, V_N as the function of iteration number, i. From Fig. 8, it is obtained that with the proper selection of the orthonormal bases to represent the linear system and the cubic spline function to represent the static nonlinear function, the cost function converges to a steady value after four iterations during the estimation process.

For comparison purposes, following the exact same identification procedure as in Sec. V, the estimation results using the 15th order polynomial function to represent the tangent nonlinear function defined in Eq. (3) is also plotted in Figs. 9a–9f. Comparing with Figs. 8b, 8c, 8e, 8f, 9b, 9c, 9e, and 9f, little difference between them can be observed. However, comparing Figs. 8d and 9d, it is easily observed that with a real hyperbolic tangent nonlinear present in the system, the estimation using cubic spline can give a better result to fit the true tangent nonlinear function, when compared with the polynomial nonlinear function. Furthermore, the cubic spline provides a much smaller oscillatory behavior at the end of the function domain compared with the polynomial function, and thus it is especially applicable for data extrapolation purposes.

VII. Conclusions

In this paper, a novel iterative identification algorithm is proposed for the estimation of the nonlinear Hammerstein model. In this algorithm, a cubic spline is applied to represent the zero memory static nonlinear function, and a linear orthonormal basis function expansion is used to represent the linear function. An iterative estimation approach is implemented to estimate the parameters of the linear and nonlinear functions of the Hammerstein model simultaneously. Using the cubic spline functions to represent the static nonlinearity can provide a better performance compared with polynomial functions, especially for signal extrapolation purposes. The advantage of using orthonormal basis expansion in orthonormal FIR filter lies in the possibility of incorporating prior poles knowledge of the system dynamics into the identification process. As a result, more accurate and simplified linear models can be obtained with a limited number of orders. With the use of the iterative estimation approach, the nonlinear Hammerstein estimation process is simplified to two standard linear least-squares estimations. Furthermore, a criterion using the frequency-domain PolyMax identification method and the stabilization diagram is applied to estimate physical poles of the dynamic system. The consistent estimation of these physical poles plays a crucial role for the generation of the orthonormal basis functions and for the model approximation results. From the estimation results of case studies, it can be concluded that the convergence rate of the iterative estimation process is very fast because of the accurate selection of the orthonormal bases; the estimation results also depend on the tuning of the orthonormal bases, which again depend on the physical pole estimation.

Acknowledgment

Research is supported by NASA Dryden Flight Research Center under the Small Business Technology Transfer Phase 2 program.

References

[1] Zhu, Y., "Identification of Hammerstein Models for Control Using ASYM," *International Journal of Control*, Vol. 73, No. 18, 2000, pp. 1692–1702. doi:10.1080/00207170050201771

[2] Westwick, D. T., and Kearney, R. E., "Separable Least Squares Identification of Nonlinear Hammerstein Models: Application to Stretch Reflex Dynamics," *Annals of Biomedical Engineering*, Vol. 29, No. 8, 2001, pp. 707–718. doi:10.1114/1.1385806

[3] Dempsey, E. J., and Westwick, D. T., "Identification of Hammerstein Models with Cubic Spline Nonlinearities," *IEEE Transactions on Biomedical Engineering*, Vol. 51, No. 2, 2004, pp. 237–245. doi:10.1109/TBME.2003.820384

[4] Baldelli, D., Lind, R., and Brenner, M., "Nonlinear Aeroelastic/Aeroservoelastic Modeling by Block-Oriented Identification," *Journal of Guidance, Control, and Dynamics*, Vol. 28, No. 5, 2005, pp. 1056–1064. doi:10.2514/1.11792

[5] Narendra, K. S., and Gallman, P. G., "An Iterative Method for the Identification of Nonlinear Systems Using a Hammerstein Model," *IEEE Transactions on Automatic Control*, Vol. 11, No. 3, 1966, pp. 546–550. doi:10.1109/TAC.1966.1098387

[6] Billings, S., and Fakhouri, S. Y., "Identification of a Class of Nonlinear Systems Using Correlation Analysis," *Proceedings of the Institution of Electrical Engineers*, Vol. 125, No. 7, 1978, pp. 691–697.

[7] Bai, E. W., "Identification of Linear Systems with Hard Input Nonlinearities of Known Structure," *Automatica*, Vol. 38, No. 5, 2002, pp. 853–860. doi:10.1016/S0005-1098(01)00281-3

[8] Previdi, F., and Lovera, M., "Identification of Non-linear Parametrically Varying Models Using Separable Least Squares," *International Journal of Control*, Vol. 77, No. 16, 2004, pp. 1382–1392. doi:10.1080/00207170412331318863

[9] Verhaegen, M., and Westwick, D., "Identifying MIMO Hammerstein Systems in the Context of Subspace Model Identification Methods," *International Journal of Control*, Vol. 63, No. 2, 1996, pp. 331–349. doi:10.1080/00207179608921846

[10] Bai, E. W., "An Optimal Two Stage Identification Algorithm for Hammerstein -Wiener Nonlinear System," *Automatica*, Vol. 34, No. 3, 1998, pp. 333–338. doi:10.1016/S0005-1098(97)00198-2

[11] Gómez, J. C., and Baeyens, E., "Identification of Block-Oriented Nonlinear Systems Using Orthonormal Bases," *Journal of Process Control*, Vol. 14, No. 6, 2004, pp. 685–697. doi:10.1016/j.jprocont.2003.09.010

[12] Ninness, B., Hjalmarsson, H., and Gustafsson, F., "The Fundamental Role of Generalized Orthonormal Basis in System Identification," *IEEE Transactions on Automatic Control*, Vol. 44, No. 7, 1999, pp. 1384–1406. doi:10.1109/9.774110

[13] Heuberger, P., Van den Hof, P. M. J., and Wahlberg, B., *Modeling and Identification with Rational Orthogonal Basis Functions*, Springer-Verlag, New York, 2005, pp. 63–100.

[14] Wahlberg, B., "System Identification Using Laguerre Models," *IEEE Transactions on Automatic Control*, Vol. 36, No. 5, 1991, pp. 551–562. doi:10.1109/9.76361

[15] Wahlberg, B., "System Identification Using Kautz Models," *IEEE Transactions on Automatic Control*, Vol. 39, No. 6, 1994, pp. 1276–1282. doi:10.1109/9.293196

[16] Ninness, B., and Gustafsson, F., "A Unifying Construction of Orthonormal Bases for System Identification," *IEEE Transactions on Automatic Control*, Vol. 42, No. 4, 1997, pp. 515–521. doi:10.1109/9.566661

[17] Heuberger, P., Van den Hof, P., and Bosgra, O. H., "A Generalized Orthonormal Basis for Linear Dynamical Systems," *IEEE Transactions*

on Automatic Control, Vol. 40, No. 3, 1995, pp. 451–465. doi:10.1109/9.376057

[18] Zeng, J., and de Callafon, R. A., "Recursive Filter Estimation for Feedforward Noise Cancellation with Acoustic Coupling," *Journal of Sound and Vibration*, Vol. 291, Nos. 3–5, 2006, pp. 1061–1079. doi:10.1016/j.jsv.2005.07.016

[19] Zeng, J., and de Callafon, R. A., "Model Matching and Filter Design Using Orthonormal Basis Functions," *45th IEEE Conference on Decision and Control*, Inst. of Electrical and Electronics Engineers, Piscataway, NJ, 2006, pp. 5347–5352.

[20] Baldelli, D. H., Zeng, J., Lind, R., and Harris, C., "Robust Flutter Prediction for Data-Based Aeroelastic LPV Models," AIAA Atmospheric Flight Mechanics Conference and Exhibit, AIAA Paper 2007-6301, Hilton Head, SC, 2007.

[21] Cauberghe, B., Guillaume, P., Verboven, P., Parloo, E., and Vanlanduit, S., "A Poly-Reference Implementation of the Maximum Likelihood Complex Frequency-Domain Estimator and Some Industrial Applications," 22nd International Modal Analysis Conference, Society for Experimental Mechanics Paper 179, Jan. 2004.

[22] Cauberghe, B., Guillaume, P., Verboven, P., Vanlanduit, S., and Parloo, E., "On the Influence of the Parameter Constraint on the Stability of the Poles and the Discrimination Capabilities of the Stabilization Diagrams," *Mechanical Systems and Signal Processing*, Vol. 19, No. 5, 2005, pp. 989–1014. doi:10.1016/j.ymssp.2004.07.007

[23] Bai, E. W., and Li, D., "Convergence of the Iterative Hammerstein System Identification Algorithm," *IEEE Transactions on Automatic Control*, Vol. 49, No. 11, 2004, pp. 1929–1939. doi:10.1109/TAC.2004.837592

[24] Bauer, D., and Ninness, B., "Asymptotic Properties of Least-Squares Estimates of Hammerstein-Wienner Models," *International Journal of Control*, Vol. 75, No. 1, 2002, pp. 34–51. doi:10.1080/00207170110091119

[25] Ninness, B., and Gibson, S., "Quantifying the Accuracy of Hammerstein Model Estimation," *Automatica*, Vol. 38, No. 12, 2002, pp. 2037–2051. doi:10.1016/S0005-1098(02)00101-2

[26] O'Neil, T., and Strganac, T., "Aeroelastic Response of a Rigid Wing Supported by Nonlinear Springs," *Journal of Aircraft*, Vol. 35, No. 4, 1998, pp. 616–622.